

# Improved Sliding Mode Control for Airborne Electro-Optical Stabilized Platforms Based on Disturbance Observer

Mengchen Yan

College of Electronic and Information Engineering/Integrated  
Circuits  
Guangxi Normal University, GXNU  
Guilin, China  
ymc@stu.gxnu.edu.cn

Rijun Wang\*

Teachers College for Vocational and Technical Education  
Guangxi Normal University, GXNU  
Guilin, China

\* Rijun Wang: wangrijun1982@126.com

Xiangwei Mou

Teachers College for Vocational and Technical Education  
Guangxi Normal University, GXNU  
Guilin, China  
xwmou@mailbox.gxnu.edu.cn

Juan Hu

College of Electronic and Information Engineering/Integrated  
Circuits  
Guangxi Normal University, GXNU  
Guilin, China  
hujian@stu.gxnu.edu.cn

**Abstract**—To address low control accuracy, long adjustment times, and disturbances such as external interference and internal parameter variations, this paper proposes an Improved Non-Singular Fast Terminal Sliding Mode Control (I-NFTSMC) algorithm based on a disturbance observer. The algorithm estimates and compensates for unknown disturbances in real-time and introduces a time-varying switching gain to reduce chattering from high-frequency switching. Simulation results show that the I-NFTSMC algorithm improves response speed by approximately 42% and reduces rise time by about 44% under disturbance conditions compared to traditional methods. This approach achieves overshoot-free and accurate tracking of input commands, significantly enhancing the stability and disturbance rejection capabilities of airborne electro-optical platforms.

**Keywords**—Stabilized Platforms; Improved Sliding Mode Control; Disturbance Observer

## I. INTRODUCTION

With advancements in the industry, multirotor unmanned aerial vehicles (UAVs) are recognized for their significant potential in both military and civilian applications [1]. The integration of electro-optical platform systems on UAVs enhances flight control precision and expands operational capabilities. However, the stability of these platforms is susceptible to various disturbances, which can lead to distortions in electro-optical data, such as image jitter, blurring, and loss of target visibility [2]. Therefore, effective control of the electro-optical platform is essential for successful target tracking [3]. Current control methods for stabilizing airborne electro-optical platforms primarily involve double closed-loop PID controls [4], which are favored for their simplicity and ease of design. However, as technology evolves, these traditional methods face significant limitations. Reference [5] proposes a self-tuning PID algorithm that utilizes fuzzy control to address model uncertainties and external noise, but it heavily relies on the design of rule sets and membership functions.

Reference [6] introduces a BP neural network for tuning key parameters in Active Disturbance Rejection Controllers (ADRC), though this approach may lead to overfitting and requires extensive tuning. Reference [7] develops a model predictive control algorithm for a three-axis gimbal, which encounters challenges such as instability during system identification and increased computational complexity. Reference [8] explores an SMC-based ADRC method aimed at enhancing servo motor accuracy against disturbances, where ADRC improves robustness, but the design of controller bandwidth significantly influences tracking error.

To address the aforementioned issues, this paper proposes an Improved Non-Singular Fast Terminal Sliding Mode Control (I-NFTSMC) algorithm. This method uses a nonlinear observer to estimate and compensate for external disturbances and employs a time-varying switching gain, designed as an exponentially decaying function based on disturbance estimation. This design enables the system to stabilize quickly while significantly reducing chattering.

## II. MATHEMATICAL MODEL OF THE ELECTRO-OPTICAL PLATFORM

The airborne electro-optical platform is mounted on the UAV via a base and is generally classified into two degrees of freedom (DOF) and three degrees of freedom[9]. It is assumed that the axes of all three frames intersect at the center of mass of the entire frame system. Due to the strong coupling between the channels, the overall design is quite complex, so the three channels are treated as independent subsystems[10]. Among them, the stability of the pitch frame, which supports the camera, has the most significant impact on image quality. Assuming the airborne gimbal is a rigid body, the nonlinear equations of the system align with those of a single-joint mechanism[11]. The dynamic equation of the pitch frame is as follows:

$$\ddot{\theta} + \frac{K_m C_e}{JR} \dot{\theta} = K_u \frac{K_m}{JR} U - \frac{T_d}{J}. \quad (1)$$

Where  $U$  is the control input,  $R$  is the armature resistance,  $K_m$  is the motor torque coefficient,  $C_e$  is the back electromotive force coefficient,  $K_u$  is the PWM power amplification coefficient, and  $J$  is the load moment of inertia.

Let  $x_1 = \theta, x_2 = \dot{\theta}$ . Considering the impact of internal parameter perturbations on the entire system, the above equation can be rewritten in state-space form as follows:

$$\begin{cases} \dot{x}_1 = x_2, \\ \dot{x}_2 = ax_2 + bU + D. \end{cases} \quad (2)$$

In equation (2),  $a = -\frac{K_m C_e}{JR}$ ,  $b = K_u \frac{K_m}{JR}$ , and  $D$  represents the lumped disturbance, which includes model parameter uncertainties and external disturbances.

The control objective of the entire airborne electro-optical platform is to maintain the stability of the line of sight. the goal is to design the control input  $U$  such that as time approaches infinity,  $\theta \rightarrow \theta_d$ .

### III. CONTROLLER DESIGN

To compensate for unknown disturbances and achieve control objectives, this paper employs an improved sliding mode control method based on a nonlinear disturbance observer. This method estimates and compensates for disturbances using a nonlinear disturbance observer. The estimated values are used to counteract the uncertainties of the lumped disturbances, thereby enhancing the stability of the control system. The control structure of the system is shown in Fig. 1.

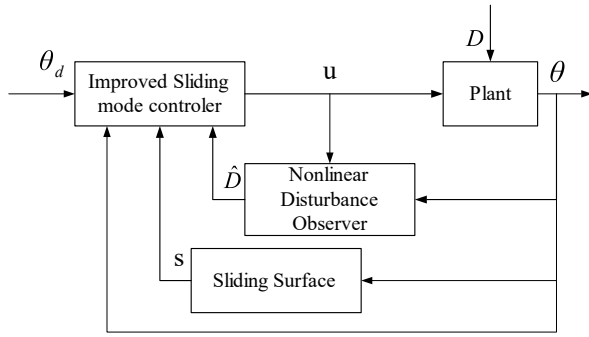


Figure 1. Sliding Mode Control Block Diagram Based on Disturbance Observer

#### A. Design of the Nonlinear Disturbance Observer

The nonlinear disturbance observer is used to estimate unknown lumped disturbances and obtain the estimated value of the lumped disturbance  $\hat{D}$ . Based on equation (1), a nonlinear disturbance observer can be designed as follows[12]:

$$\begin{cases} \dot{P} = -lP - l(lx_2 + ax_2 + bu), \\ \hat{D} = P + lx_2. \end{cases} \quad (3)$$

$l$  is the observer gain for the design of the observer,  $\hat{D}$  is the estimated value of the disturbance obtained through the observer, and  $P$  represents the state of the disturbance observer.

Define  $\tilde{D} = D - \hat{D}$  as the error between the actual value and the estimated value of the disturbance.

Assuming that the external disturbance changes very slowly or is a constant, we can have  $\dot{D} = 0$ .

Next, taking the derivative of  $\tilde{D}$  yields:

$$\begin{aligned} \dot{\tilde{D}} &= \dot{D} - \dot{\hat{D}} = -\dot{P} - l\dot{x}_2 \\ &= lP + l(lx_2 + ax_2 + bu) - l\dot{x}_2 \\ &= l(\hat{D} - lx_2) + l(lx_2 + ax_2 + bu - ax_2 - bu - D) \\ &= l(\hat{D} - D) = -l\tilde{D}. \end{aligned} \quad (4)$$

Design the Lyapunov function as:

$$V = \frac{1}{2} \tilde{D}^2. \quad (5)$$

Taking the derivative of the Lyapunov function and substituting equation (4) into it, we obtain:

$$\dot{V} = \tilde{D} \dot{\tilde{D}} = -l\tilde{D}^2. \quad (6)$$

The convergence rate of the observer is related to  $l$ . we only need to design  $l > 0$  to satisfy the Lyapunov stability condition,

#### B. Sliding Mode Controller Design

Sliding mode control is recognized for its robustness and anti-disturbance capabilities, as the design of the sliding mode surface is independent of the controlled system's parameters and external disturbances. This paper adopts sliding mode control as the primary method.

Let  $e = x_1 - x_d$ ,  $\dot{e} = \dot{x}_1 - \dot{x}_d$ , and  $\ddot{e} = \ddot{x}_1 - \ddot{x}_d$ , where  $x_d$  represents the desired angle.

Therefore, the non-singular fast terminal sliding mode surface designed in this paper is:

$$s = e + \frac{1}{\alpha} e^{g/h} + \frac{1}{\beta} \dot{e}^{p/q} \quad (7)$$

In the equation,  $\alpha, \beta > 0$ ,  $q < p < 2q$ ,  $\frac{g}{h} > \frac{p}{q}$ , and  $g, h, q, p$  are positive odd integers.

Taking the derivative of the sliding mode surface, we can obtain:

$$\dot{s} = \dot{e} + \frac{g}{\alpha h} e^{g/h-1} \dot{e} + \frac{p}{\beta q} \dot{e}^{p/q-1} \ddot{e}. \quad (8)$$

Since the switching gain of sliding mode control can cause chattering near the sliding surface, the larger the switching gain, the more pronounced the chattering. In this paper, combining the disturbance estimate  $\hat{D}$  from the disturbance observer, a novel sliding mode control law can be designed as:

$$\begin{cases} U = \frac{1}{b} \left[ \begin{aligned} &-\frac{\beta q}{p} \left( 1 + \frac{g}{\alpha h} e^{\frac{g}{h}-1} \right) \dot{e}^{2-\frac{p}{q}} + \ddot{x}_d - \\ &ax_2 - \hat{D} - (\epsilon + \text{sgn}(\hat{D})\gamma) \text{sgn}(s) \end{aligned} \right] \\ \dot{\gamma} = -k\gamma + N, \quad \gamma(0) = F. \end{cases} \quad (9)$$

We define  $\text{sgn}(\hat{D})$  as:

$$\text{sgn}(\hat{D}) = \begin{cases} 0, & \hat{D}(t) = 0. \\ 1, & \hat{D}(t) \neq 0. \end{cases} \quad (10)$$

### C. Stability Analysis

To prove that the closed-loop system is stable under the new control law, define the Lyapunov function as:

$$V = \frac{1}{2}s^2. \quad (11)$$

Taking the derivative, we obtain:

$$\begin{aligned} \dot{V} &= s\dot{s} = s\left(\dot{e} + \frac{g}{ah}e^{g/h-1}\dot{e} + \frac{p}{\beta q}\dot{e}^{p/q-1}\ddot{e}\right) \\ &= s\left(\dot{e} + \frac{g}{ah}e^{g/h-1}\dot{e} + \frac{p}{\beta q}\dot{e}^{p/q-1}(ax_2 + bU + D - \ddot{x}_d)\right) \end{aligned} \quad (12)$$

Substituting equation (9) into equation (12), we obtain:

$$\begin{aligned} \dot{V} &= s[D(t) - \hat{D}(t) - (\epsilon + \text{sgn}(\hat{D})\gamma)\text{sgn}(s)] \\ &= s[-(\epsilon + \text{sgn}(\hat{D})\gamma)\text{sgn}(s) + \tilde{D}] \\ &\leq -(\epsilon + \text{sgn}(\hat{D})\gamma)|s| + \tilde{D}|s| \\ &\leq -\epsilon|s| - \text{sgn}(\hat{D})\gamma|s| + \tilde{D}|s|. \end{aligned} \quad (13)$$

Since the formula  $\text{sgn}(\hat{D})$  exists, we will discuss two cases separately.

Case 1: When there are no external disturbances,  $D = 0$ . Through the disturbance observer, we obtain  $\hat{D} = 0$ . Based on our definition of  $\text{sgn}(\hat{D})$  and  $\tilde{D}$  we have  $\text{sgn}(\hat{D}) = 0$  and  $\tilde{D} = 0$ . Substituting these into the above equation yields:

$$\dot{V} \leq -\epsilon|s|. \quad (14)$$

Case 2: When external disturbances are present,  $D \neq 0$ . Through the disturbance observer, we obtain  $\hat{D} \neq 0$ . Based on equations (4) and (9), we can derive equation (15).

$$\begin{cases} \tilde{D} = e^{-lt}\tilde{D}(0), & \tilde{D}(0) = D(0) - \hat{D}(0), \hat{D}(0) = 0, \\ \gamma = e^{-kt}\gamma(0) + e^{-kt}\int Ne^{kt}dt, & \theta(0) = F. \end{cases} \quad (15)$$

Substituting equation (15) into equation (13), we can obtain:

$$\begin{aligned} \dot{V} &\leq -\epsilon|s| - [e^{-kt}\gamma(0) + e^{-kt}\int Ne^{kt}dt - e^{-lt}\tilde{D}(0)]|s| \\ &\leq -\epsilon|s| - e^{-kt}F|s| - e^{-kt}\int Ne^{kt}dt|s| + e^{-lt}|D(0)||s| \\ &\leq -\epsilon|s| - e^{-kt}F|s| + e^{-lt}F|s| - e^{-kt}\int Ne^{kt}dt|s| \\ &\leq -\epsilon|s|. \end{aligned} \quad (16)$$

Based on the above analysis, according to the Lyapunov stability condition, whether in the presence of disturbances or not, we can conclude that the error can reach the sliding mode surface within a finite time, thereby proving that the designed control law can stabilize the entire system.

Although the traditional sliding mode control combined with a disturbance observer exhibits strong robustness to uncertainties and disturbances, it often leads to chattering. This chattering can cause frequent switching of control inputs, resulting in degraded system performance. The novel control strategy proposed in this paper ensures robustness while reducing chattering, making it more advantageous when dealing with external disturbances and parameter uncertainties.

## IV. SIMULATION AND ANALYSIS

To verify the effectiveness of the method proposed in this paper, this section conducts simulation validation using MATLAB. The direct current torque motor used in a certain

signal machine's airborne optoelectronic platform has an armature resistance of  $7.77\Omega$ , a torque coefficient  $K_m$  of 6, an electromotive force coefficient  $C_e$  of 1.2, an amplification factor  $K_u$  of 11, and a load moment of inertia  $J$  of  $0.6 \text{ kg}\cdot\text{m}^2$ . The parameters of the sliding mode surface are chosen as  $\alpha = 3$ ,  $\beta = 5$ ,  $g = 5$ ,  $h = 3$ ,  $q = 5$ ,  $p = 7$ , with a sliding mode switching gain  $\epsilon = 1.5$  and a disturbance observer gain  $l = 100$ . To demonstrate the advantages of the method proposed in this paper, comparative experiments will be conducted with traditional sliding mode control algorithms, and the simulation results are presented below.

### A. Step Response

The step response can significantly reflect the dynamic characteristics of the system. First, the initial angular position of the airborne optical stabilization platform is set to 0, with the initial angular velocity also at 0, and the reference signal is defined as a unit step response signal. The tracking curves and error curves for the traditional sliding mode control and the I-NFTSMC control method are shown in Fig.2 and Fig.3, respectively.

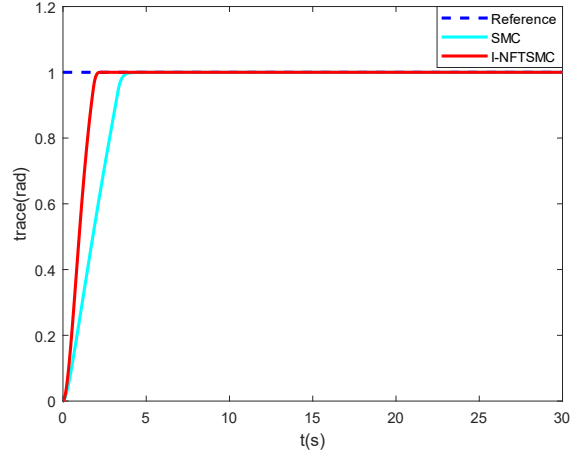


Figure 2. Tracking Simulation of Step Response

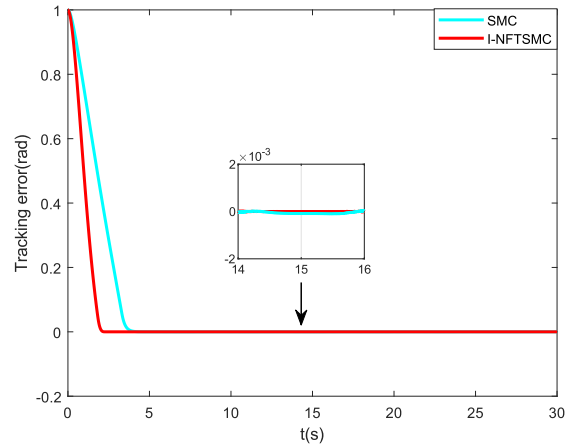


Figure 3. Error Tracking Curve of Step Response

In the step response simulation test, due to the presence of initial error, the proposed improved non-singular fast terminal

sliding mode control based on a disturbance observer achieves a tracking error convergence to 0 in 2.08 seconds. In contrast, the traditional sliding mode control takes 3.63 seconds for the error to converge to 0. This indicates that the I-NFTSMC control method exhibits a faster response speed to step signals. According to the trajectory tracking error graph, both control methods show no overshoot. The improved sliding mode control method reduces the settling time by approximately 42% and the rise time by about 44% compared to the traditional sliding mode control method.

### B. Disturbance Rejection Experiment Simulation

To verify the disturbance rejection capability and tracking response of the designed controller, dynamic interference  $0.1\sin(\pi t)$  and friction torque were added to the model, and the command signal was changed to a sinusoidal tracking signal  $\theta_d = \sin(0.5t)$ . The simulation results are shown in the Fig. 4 and Fig.5. From the figures, it can be observed that under the control method combining NDOB and I-NFTSMC, the airborne optical stabilization platform can fully track the command signal in real time, with a very small steady-state tracking error. Compared to traditional sliding mode control and fixed switching gain methods, the proposed method exhibits a faster response speed, and as shown in Fig.6, the disturbance observer error remains within 2 mrad.

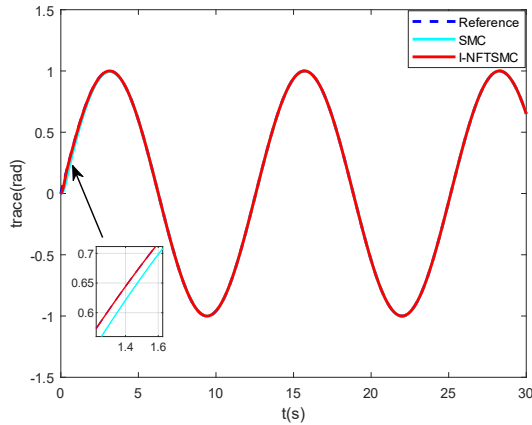


Figure 4. Sine Input Tracking Curve

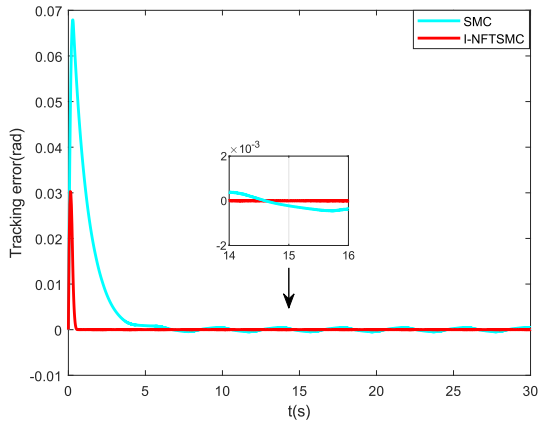


Figure 5. Sine Input Tracking Error Curve

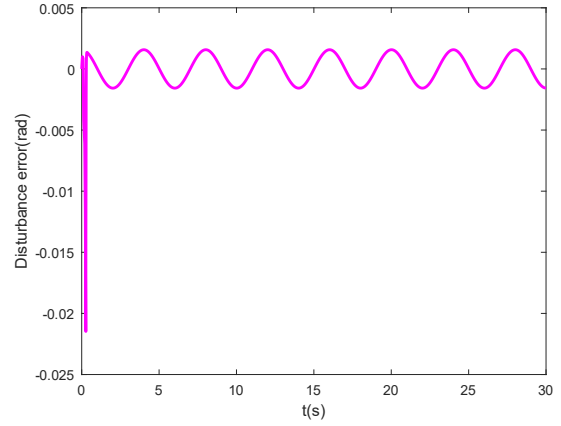


Figure 6. Disturbance Observer Observation Error

## V. CONCLUSIONS

In response to the susceptibility of airborne electro-optical platforms to external disturbances and the strong nonlinearity of the controlled object, this paper adopts a control method that combines disturbance observation with I-NFTSMC. The theoretical explanation and simulation results demonstrate that the disturbance observer can effectively estimate and compensate for the impact of total disturbances on system control. By leveraging the robustness of nonsingular fast terminal sliding mode control, the stability of the system can be further ensured. The switching gain is designed as an exponentially decaying function, leading to the construction of an improved sliding mode control rate. This novel control rate design reduces chattering and shortens the time to reach a stable state compared to traditional sliding mode control methods.

## ACKNOWLEDGMENT

This work was supported by the Science and Technology Planning Project of Chongzuo (No. 2023XC035676), the Science and Technology Planning Project of Guangxi Province, China (No. AD23026273), and the Industry-University-Research Innovation Fund Projects of China University in 2021 (No. 2021ITA10018).

## REFERENCES

- [1] Brake N J. Control system development for small uav gimbal[D]. California Polytechnic State University, 2012.
- [2] Huilin W, Fei N, Jilong L I U. Development of aviation electro-optical reconnaissance technology[J]. Journal of Applied Optics, 2022, 43(5): 825-832.
- [3] Lee D H, Tran D Q, Kim Y B, et al. A robust double active control system design for disturbance suppression of a two-axis gimbal system[J]. Electronics, 2020, 9(10): 1638.
- [4] M. H. Ahmad, K. Osman, M. F. M. Zakeri and S. I. Samsudin, "Mathematical Modelling and PID Controller Design for Two DOF Gimbal System," 2021 IEEE 17th International Colloquium on Signal Processing & Its Applications (CSPA), Langkawi, Malaysia, 2021, pp. 138-143.
- [5] Şahin M. Stabilization of Two Axis Gimbal System with Self Tuning PID Control[J]. Politeknik Dergisi, 2023: 1-1.
- [6] Niazi S, Toloei A, Ghasemi R. Neuro-Predictive Controller for Stabilization of Gimbal Mechanism with Cross-Coupling[J]. Mechatron. Syst. Control, 2021, 49: 2021.201-0198. (references)

- [7] Altan A, Hacıoğlu R. Model predictive control of three-axis gimbal system mounted on UAV for real-time target tracking under external disturbances[J]. Mechanical Systems and Signal Processing, 2020, 138: 106548.
- [8] Zhao L, Shi Y. Disturbance Suppression of Gimbal Servo Motor Based on Improved ADRC and ISMC Method[J]. Journal of Electrical Engineering & Technology, 2024: 1-11.
- [9] Guo Q, Liu G, Xiang B, et al. Robust control of magnetically suspended gimbals in inertial stabilized platform with wide load range[J]. Mechatronics, 2016, 39: 127-135.
- [10] Tiimus K, Tamre M. Camera gimbal control system for unmanned platforms[C]//7th International DAAAM Baltic Conference "INDUSTRIAL ENGINEERING. 2010: 22-24.
- [11] Mousavi Y, Zarei A, Jahromi Z S. Robust adaptive fractional-order nonsingular terminal sliding mode stabilization of three-axis gimbal platforms[J]. ISA transactions, 2022, 123: 98-109.
- [12] Chen W H, Yang J, Guo L, et al. Disturbance-observer-based control and related methods—An overview[J]. IEEE Transactions on industrial electronics, 2015, 63(2): 1083-1095.